

Time-to-Contact, Advances in Psychology series
Heiko Hecht & Geert J. P. Savelsbergh (Eds.)
2004 Amsterdam: Elsevier - North-Holland

CHAPTER 4

Predicting Motion: A Psychophysical Study

Lucia M. Vaina

Boston University, Boston, MA, USA
Harvard Medical School, Cambridge, MA, USA

Franco Giulianini

Boston University, Boston, MA, USA

ABSTRACT

Assad and Maunsell (1995) found neurons in the primate posterior parietal cortex (PPC) whose response seems to be tuned to the animal's inference of the motion of a visual target. These neurons maintain an appreciable response in the absence of retinal stimulation when the visual target is inferred to move behind an occluder. In the present study we investigated psychophysically the ability of human observers to predict the position of a visual target after it disappears behind an imaginary occluder by using a task similar to that by Assad and Maunsell. The accuracy of the predictions were measured psychophysically as a function of the velocity of the target and the time the target was visible by using a forced choice paradigm. The results were interpreted in the context of a simple model that reflects known properties on neurons in PPC.

1. Introduction

The 2-dimensional retinal images of objects and surfaces that make up our visual environment are affected by a high degree of spatio-temporal discontinuity due to the occlusions of objects and surfaces with each other. Occlusion is an obvious consequence of the fact that we live in a 3-dimensional world. However, despite the fragmented nature of the retinal images our visual system is capable to “unconsciously infer” (Helmoltz, 1910) the parts of an object that are occluded by another object, thus preserving its continuity and integrity. The inference of parts of objects that are occluded in space by another object is referred to as “amodal completion” (Michotte, Thines & Crabbe 1964). Amodal integration (Yantis, 1995) is the temporal analogue of amodal completion, it refers to the capability of observers to perceive an object as continuing behind a surface through time. Amodal integration occurs when a moving object is occluded for a short time by a surface: despite the absence of a retinal signal the object is still perceived as continuing behind the surface.

There is emerging evidence that the neurons in the posteriori (Assad & Maunsell, 1995; Snyder et al, 1997) parietal cortex (PPC) use extra-retinal information to infer the motion of an object that is temporally occluded by a real or imaginary occluder. Assad and Maunsell (1995), reported that neurons in PPC maintain an appreciable activity after the disappearance of a moving target that then reappears at a position consistent with the target continuously moving during the time it was not visible (like, for example, a moving object that enters and exits a tunnel). A straightforward sensory-off response could not account for this phenomenon, since almost half of these neurons were significantly more active in this task than in a condition where the target disappeared and then reappeared in the same location after some time, as if it did not move at all during the time it was not visible. The authors suggest that the difference in activity between the two tasks is related to the animal’s inference of the motion of the target. The sustained activity of these neurons may provide the neural substrate for constructing an abstract representation of the motion of a visual target. The capability to create and maintain such representation is of crucial importance for accurate and stable visual guidance, such as reaching for a moving object, motor planning, or control of driving.

By using a similar task to that of Assad and Maunsell (1995), in this study we explored psychophysically the ability of human observers to infer the motion of a visual target. The display consisted of a dot moving along a circular trajectory for a fixed time and then continuing its motion behind an imaginary occluder. Observers were asked to make judgements on the position of the dot at a time Δt after it disappeared (see 2. Methods). The measured accuracy of observers’ judgements can be explained by a simple integrator that collects the information on the target motion while it is visible.

2. Methods

2.1 Apparatus and stimuli

Stimuli were created and displayed on a Macintosh computer (832 x 624 pixels resolution, 75 Hz screen refresh rate). The display consisted of a 0.24° diameter white dot that moved along a black circular trajectory 8° in diameter (see Figure 1a) at a constant angular velocity. The circle was displayed

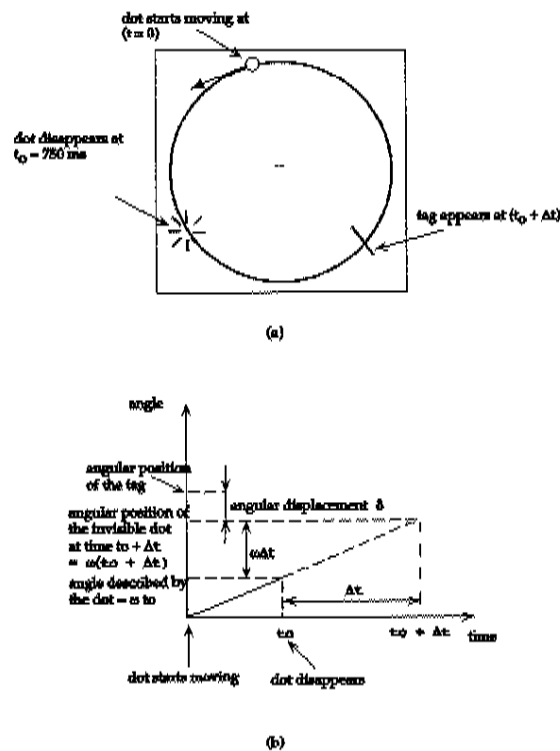


Figure 1: (a) Stimulus set up: the circular trajectory is 8° diameter, the fixation square in the center of the circle is 0.4° wide and the moving dot is 0.24° in diameter. (b) Experimental procedure: the dot moves for t_0 before disappearing. After a time Δt , a tag is displayed on the circumference. The tag is displaced from the position where the dot should be by \pm a displacement angle σ , which is adaptively adjusted from trial to trial (see text). The observer's task is to report whether the dot is ahead of or beyond the tag.

throughout the entire experimental run. A circular trajectory permits to keep the eccentricity of the moving dot constant, avoiding the complications resulting from retinal inhomogeneity for motion sensitivity with eccentricity. Observers were instructed to fixate the center of the display indicated by a white 0.4° wide white square. Viewing distance was 60 cm, the angular velocities used in the experiment ranged from 37 deg/sec to 131deg/sec. Angular velocity is expressed in degrees/sec, where "degrees" refer to angles measured on the monitor screen with respect to the center of the circle (not visual angle).

2.2 Procedure

The basic experimental procedure is schematically illustrated in Figure 1b. At time $t = 0$, the dot starts moving in counter-clockwise direction along the circle with angular velocity ω and, after a time t_0 , it suddenly disappears. The observer is asked to assume that while the dot is not visible it continues to move as if it were behind an imaginary occluder. After a time interval Δt , a small tag appears perpendicular to the circle (see Figure 1a & b) and the observer's task is to judge whether the invisible dot is ahead of or behind the tag by pressing one of two keys. In each trial, the tag is randomly placed ahead of or behind the position where the dot should be. During the experimental run the amount of displacement is determined by an adaptive staircase, which automatically terminates when nine reversals are reached. The staircase increases the angular displacement σ (see Figure 1b) after one incorrect response and decreases it after three consecutive correct responses. This procedure tracks the 74% correct response level of the psychometric function (Wetherill & Levitt, 1965). The step sizes are linearly spaced within each decade of the staircase. The "minimum detectable displacement angle" (mdda) estimated in a single experimental run was the mean of the last six reversals. The data reported show mean and standard error based upon six independent runs (i.e. the standard error plotted reflects between-runs variability). The measured mdda is an estimate of the observer's uncertainty on the angular position of the moving dot at the time Δt after it is no longer visible. The observer can only tell that the invisible dot is somewhere between " $\omega(\Delta t + t_0)$ (position where the dot should be) \pm mdda" (see Figure 1b). Two different Δt s were used: 1250 and 1850 ms. At the beginning of each trial the dot initiated its motion from a randomly chosen position on the circle. Three observers participated in the experiment, one of the authors (FG) and two naive observers (MI and DH). Mddas were measured for two different conditions: (i) the time the dot is visible (t_0) and the time it is occluded (Δt) were kept constant while the angular velocity ω was varied and (ii) ω and Δt were kept constant while t_0 was varied.

In the experiments reported here, the observers were asked to predict the position of the dot that disappears behind an imaginary occluder. The effect of a real occluder, like a surface defined by illusory contours (Kanizsa, 1979), on the accuracy of predictions will be measured in a future experiment.

2.3 Results and model

2.3.1 Results

Figures 2a & b show mddas from two observers measured as a function of angular velocity ω , for $\Delta t = 1250$ ms (filled symbols) and $\Delta t = 1850$ ms (open symbols). The graphs in Figure 2 show that for both observers the uncertainty on the angular position of the dot increases linearly with angular velocity. The uncertainties in the angular positions of the dot are higher for the longer Δt . The lines in the figure represent the best least-square fit to the data of the "mdda = $m\omega$ " line. As we will elaborate in the next section, these lines represent the predictions of a simple integrator model and the slope "m" can be related to the time-decay parameter τ of the model (see next section). For observer FG the slopes are:

$m_{1250} = 0.23$ (the correlation r between data and the predictions of the best fitting line is 0.97), $m_{1850} = 0.37$ ($r = 0.94$). For observer MI: $m_{1250} = 0.27$ ($r = 0.99$) and $m_{1850} = 0.39$ ($r = 0.96$).

Figures 3a & b illustrate the data from two observers (DH and FG) for the condition in which the mddas were measured as a function of t_0 (the time during which the moving dot was visible). The angular velocity was fixed at 75 deg/sec, Δt was 1250 ms and t_0 varied between 200 and 1750 ms. The plots show relative uncertainties, that is "mdda / α " where $\alpha = \omega \Delta t$. For both observers, the relative uncertainty did not vary with the time t_0 . The horizontal dotted lines in Figure 3 represent the mean relative uncertainty for the two observers.

The data presented in Figures 2 and 3 are consistent with the predictions of an integrator model discussed in the next section.

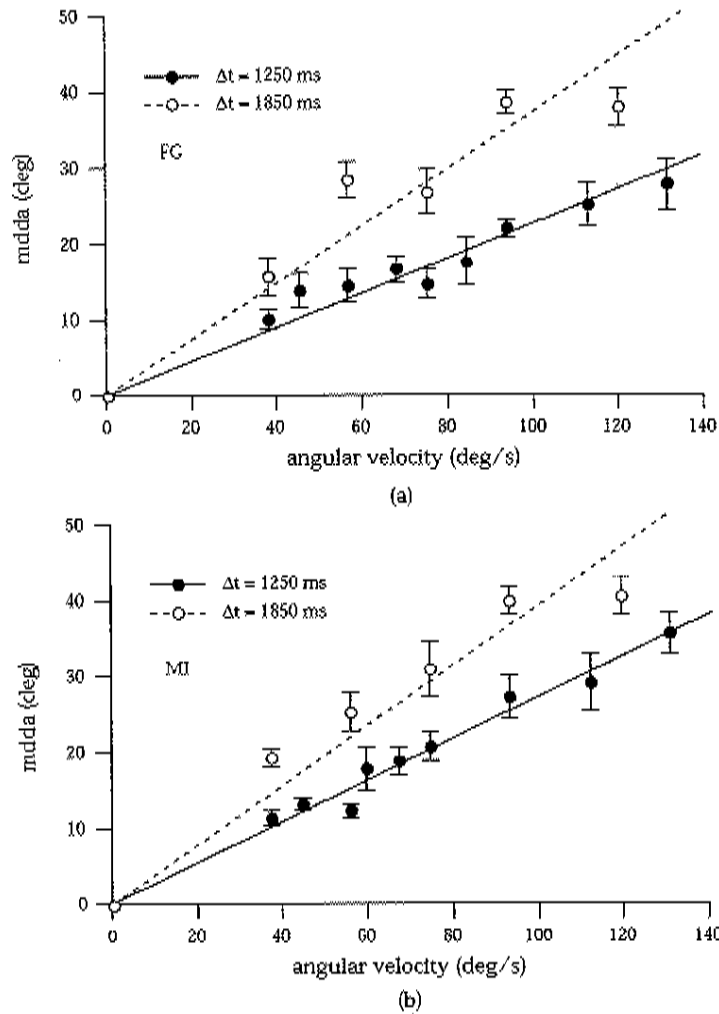


Figure 2: Mdda as a function of angular velocity for observers FG and MI. The time the dot is visible was kept constant at 750 ms and two different Δt s were used: 1250 ms (solid symbols) and 1850 ms (open symbols). (a) Data from observer FG. (b) Data from observer MI. For both observers the "mdda" increases linearly with angular velocity. The dotted lines represent the best fitting model to the data (see text).

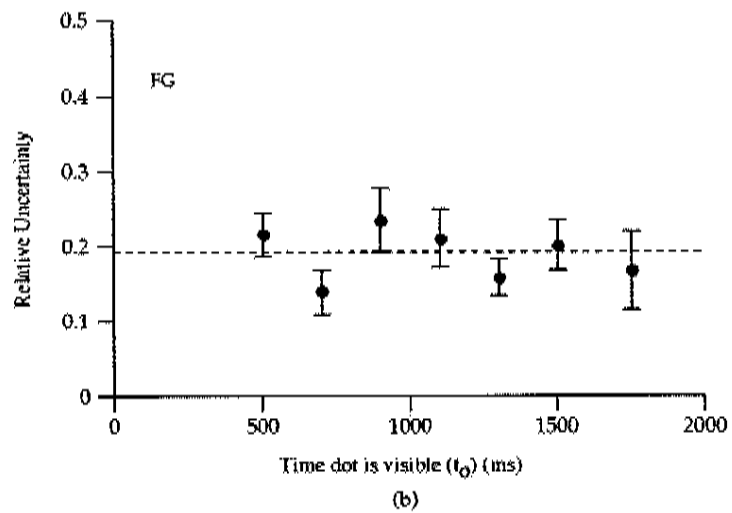
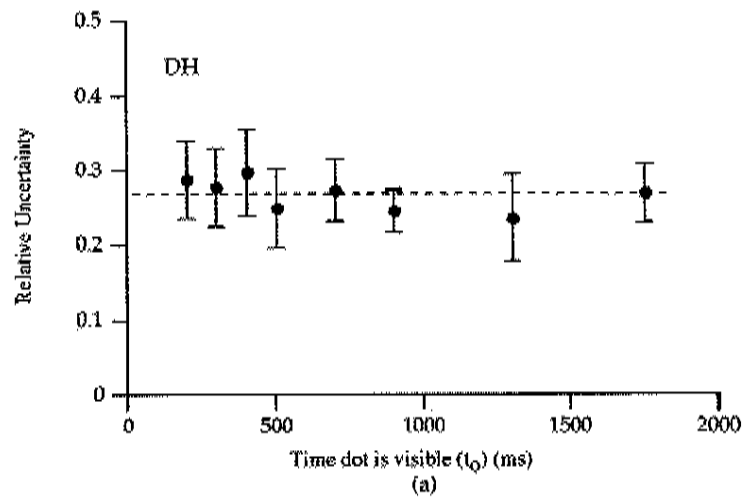


Figure 3: Relative uncertainty as a function of the time the dot is visible (t_0) for observers HD (a) and FG (b). The angular velocity is fixed at 75 deg/sec and $\Delta t = 1250$ ms.

2.3.2 Model

Figure 4 illustrates the integrator model used to interpret the psychophysical data. The model involves two distinct sequential processes: (i) a build-up process during which the visual system collects and integrates the information about the motion of the dot and (ii) a decay process during which such information extinguishes. The basic architecture of the model consists of a group of motion selective units that respond to the velocity of the dot in the Middle Temporal (MT) area (Maunsell & Van Essen, 1983) and a neural unit, presumably in PPC, that integrates the signals collected by the MT neurons.

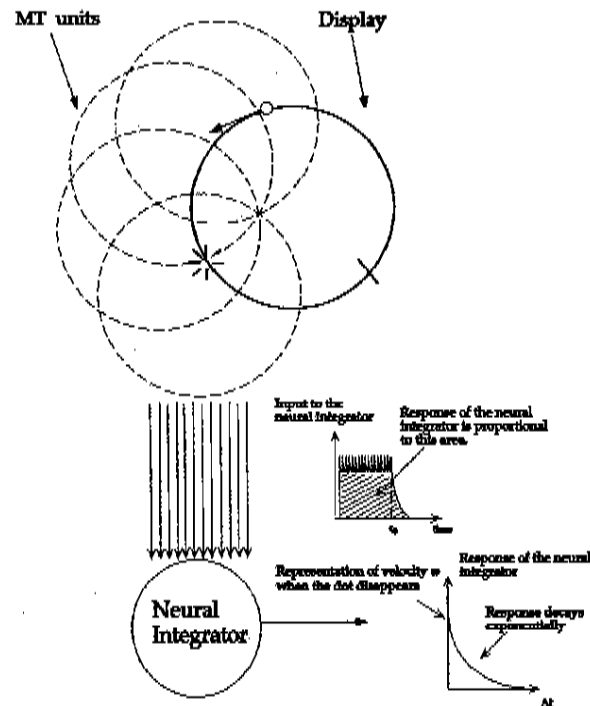


Figure 4: Schematic representation of the model used to interpret the psychophysical data. A group of MT units respond to the moving dot. The signals from these neurons are the input to a neural integrator. The response of the integrator is proportional to the angular distance covered by the dot during the time t_0 while it is visible and provides a neural representation of the velocity of the target. Such representation decays exponentially with time.

The higher the angular velocity of the dot, the larger the angle it runs and, consequently, the larger the signal collected and integrated during the time the dot is visible. Since this signal is proportional to the angle covered by the dot's motion during the time t_0 while it is visible, we suggest that it provides a representation of the angular velocity ω of the moving dot. Immediately after the moving dot becomes invisible, the strength of this representation decays exponentially with time constant τ .

The linking hypothesis between the behavior of the model and the observers' performance is that when, at time Δt after the dot disappears, observers make a judgment on the angular position of the dot, their response is based on the accuracy of the representation of the angular velocity at the decision time. The observers' uncertainty $\Delta\omega$ in judging the angular velocity of the target is reflected in the psychophysically measured mddas.

Let ω_0 be the angular velocity of the dot. We can formulate the model as follows: at time t_0 , when the dot disappears, the neural integrator has collected a signal proportional to ω_0 . Immediately after the dot disappears, the signal starts to decay exponentially and so does the representation of the angular velocity:

$$\omega(\Delta t) = \omega_0 e^{-\frac{\Delta t}{\tau}},$$

where τ is the time constant that characterizes the decay process. The model assumes that immediately after the dot disappears, that is for $\Delta t = 0$, the observer has no uncertainty on the angular velocity of the target and that her/his uncertainty increases with Δt . The observer's uncertainty $\Delta\omega$ as a function of Δt , can then be expressed as:

$$\Delta\omega(\Delta t) = \omega_0 - \omega_0 e^{-\frac{\Delta t}{\tau}} = \omega_0 (1 - e^{-\frac{\Delta t}{\tau}}) \quad (1)$$

From (1) we have that at $\Delta t = 0$, $\Delta\omega = 0$ (i.e. no uncertainty) and for $\Delta t \rightarrow \infty$, $\Delta\omega = \omega_0$. The latter defines the level of total uncertainty of the observer: when $\Delta\omega = \omega_0$, the observer's estimate of the angular velocity of the target is " $\omega_0 \pm \omega_0$ ", in other words the observer cannot tell whether the target is moving or not.

From equation (1), we can obtain the observer's uncertainty on the angular position of the dot (when its motion is masked by an illusory occluder) as a function of Δt :

$$\Delta\alpha(\Delta t) = \Delta\omega(\Delta t) \cdot \Delta t = \omega_0 \Delta t (1 - e^{-\frac{\Delta t}{\tau}}) = \alpha (1 - e^{-\frac{\Delta t}{\tau}}) \quad (2)$$

where $\alpha = \omega_0 \Delta t$. $\Delta\alpha$ is the "minimum detectable displacement" measured in our experiment.

Equation 2 makes three predictions: (i) for a fixed value of Δt there should be a linear relationship between angular uncertainty on the dot position

and angular velocity; (ii) for a fixed value of ω the uncertainty on the angular position should increase with Δt (since $\Delta t (1 - \exp(-\Delta t/\tau))$ is a monotonically increasing function of Δt); (iii) the relative uncertainty $\Delta\alpha/\alpha$ does not depend on t_0 and is constant for a given value of Δt and τ .

These predictions are qualitatively confirmed by the experimental data shown in Figures 2 and 3. For both observers, the data in Figure 2 illustrate a clear linear relationship between uncertainty in angular position and angular velocity (prediction (i)), the angular uncertainties are larger for $\Delta t = 1850$ ms (prediction (ii)) and Figure 3 shows that the relative uncertainty on the angular position of the dot does not depend on t_0 (prediction (iii)).

The value of the time-decay parameter τ can be estimated from the data in Figure 2. The lines in Figure 2 represent the best least-square fit to the data of the $\Delta\alpha = m\omega$ line, where m is the slope. From (2), we have that $m = \Delta t (1 - \exp(-\Delta t / \tau))$, which entails that the time constant τ is related to the slope m by: $\tau = -(\Delta t / (\ln(1 - m / \Delta t)))$. Table 1 reports estimates of τ for two observers and for the two different Δt s tested.

	FG	MI
$\Delta t = 1250$ ms	$\tau = 6.15$ sec	$\tau = 5.14$ sec
$\Delta t = 1850$ ms	$\tau = 8.29$ sec	$\tau = 7.81$ sec

Table 1

Data from Figure 3 also allow to estimate τ . The dotted line in Figure 3 is drawn by equation $\Delta\alpha/\alpha = k$, where k is the mean uncertainty. From Equation (2) we have $\Delta\alpha/\alpha = (1 - \exp(-\Delta t / \tau))$. Substituting $\Delta\alpha/\alpha = k$ in this expression gives $k = (1 - \exp(-\Delta t / \tau))$ from which we get $\tau = -(\Delta t / \ln(1 - k))$.

For observer MI the mean τ , from the data in Figure 2, is $6.47 \text{ s} \pm 1.33 \text{ s}$; for FG the mean τ , from the data in Figure 2 and 3, is $6.74 \text{ s} \pm 0.78 \text{ s}$. In the context of the proposed model, this means that it takes several seconds for the observer to have an uncertainty on the angular velocity which is 63% of its initial value (when $\Delta t = \tau$, $\Delta\omega / \omega_0 = (1 - e^{-1}) = 0.63$). For observer FG, for example, a time constant of 6.74 sec means that his uncertainty on the angular velocity of the dot is about 14% of the total angular velocity after 1 second from the time the dot disappeared (for $\Delta t = 1$, $\Delta\omega / \omega_0 = (1 - e^{-1/6.74}) \approx 0.14$).

3. Discussion

The purpose of this study was to characterize psychophysically the ability of human observers to infer the motion of a moving object when it disappears behind an imaginary occluder and to relate this capability to possible neural mechanisms underlying this process. The main result of the study is that the observer's uncertainty on the position of the invisibly moving dot increases linearly with the dot's angular velocity and that the slope of the best fitting line to the data increases with the time Δt during which the dot motion is invisible (Figure 2). The second result (Figure 3) is that the relative uncertainty on the angular position of the dot is independent of the time the motion of the dot is visible (at least for values of $t_0 > 200$ ms).

We suggested that a simple neural integrator model provides a plausible neural substrate for the mechanisms mediating this task. Since MT neurons are sensitive to both speed and direction of the stimulus (Maunsell & Van Essen, 1983), they are a suitable candidate for providing the input to the integrator unit in the model. This unit creates a representation of the target motion that is presumably used by observers to make decisions on the target position. As defined previously, t_0 is the time during which the visual system can integrate the motion information. It is important to determine the critical t_0 value necessary for creating a robust representation of the target motion. In order to address this question we must measure $mddas$ for a larger range of t_0 values, including values shorter than 200 ms (the shortest t_0 used in this study). Furthermore we will also measure the minimum Δt value for which observers can make reliable predictions of the target position. Preliminary data showed that for very short Δt s (of the order of about 100 ms), observers cannot do the task. This suggests that perhaps the building up of the representation of target motion continues for some time after the retinal signal is no longer available. It is possible that, during this time, the observer cannot use the representation to make decisions on the putative position of the (invisibly moving) target. It is important to point out that while the representation of the target motion is derived from retinal information, the decision process is based on extra-retinal information. That is, when observers make a decision on the target position at time $(t_0 + \Delta t)$, the only information available is that acquired during the time t_0 (when the dot is visible).

The use of extra-retinal information is ubiquitous in PPC. This region is part of the neural pathway involved in the generation of the smooth pursuit reflex and activity in this cortical area can be modulated by attention or the intentionality of making an eye movement (Barash, Bracewell, Fogassi, Gnadt & Andersen, 1991a, b; Bushnell, Goldberg & Robinson 1981; Goldberg, Colby & Duhamel 1990). In the experiments reported here, the observers were instructed

to fixate at the center of the circular trajectory and not make eye movements. However, this would not exclude the possibility that, unconsciously, one pursues the moving dot by attentionally tracking it. The pursuit reflex is a form of predictive behaviour (Barnes, 1993) and is highly dependent on the target motion: for regular, predictable, motions (like, periodic motions or the motion used in our task) the eye - displacement follows closely the target displacement. For target motions that are not predictable the pursuit reflex performance deteriorates (Barnes, 1993). It is, thus, possible to speculate that the same information is used for inferring the target position and for regulating the pursuit response. If this were the case, smooth pursuit of the visual target should not improve significantly the accuracy of the prediction of the target position in the psychophysical task we described here. In planned experiments to compare the performance of observers in the two conditions we will specifically address this speculation.

Alternatively, it is possible that the spatial position of the target is represented more abstractly by extraretinal signals in some PPC neurons. We refer to the representation as abstract because the signals contributing to it are not sensory (the target is not visible) nor coupled with eye movements. Colby and collaborators (1995) suggested that these signals may reflect the observer's expectation that the target is at a particular spatial location or that it is moving at a specific speed, even when the target motion is actually not seen.

Acknowledgment

This work was supported in part by the NIH grant EY-2RO1-07861 to L.M.V.

REFERENCES

- Assad, J. A. & Maunsell, J. H. (1995). Neuronal correlates of inferred motion in primate posterior parietal cortex. *Nature*, 373, 518-21.
- Assad, J. A. (1998). *Personal Communication to L. M V.*
- Barnes, G. R. (1993). Visual-vestibular interaction in the control of head and eye movement: the role of feedback and predictive mechanisms. *Prog. Neurobiol.*, 41, 435-472.
- Barash, S., Bracewell, R. M., Fogassi L., Gnadt, J. W. & Andersen, R. A. (1991a). Saccade related activity in the lateral intraparietal area. I. Temporal properties. *Journal of Neurophysiology* 66, 1176-1196.
- Barash, S., Bracewell, R. M., Fogassi L., Gnadt, J. W. & Andersen, R. A., (1991b). Saccade related activity in the lateral intraparietal area. II Spatial properties. *Journal of Neurophysiology*, 66, 1176-1196.
- Bushnell, M. C., Goldberg, M. E. & Robinson, D. L. (1981). Behavioural enhancement of visual responses in monkey cerebral cortex. I. Modulation in posterior parietal cortex related to selective visual attention. *Journal of Neurophysiology*, 46, 755-772.
- Colby, C. L., Duhamel, J. & Goldberg, M. E. (1995). Oculocentric spatial representation in parietal cortex. *Cerebral Cortex*, 5, 470-481.
- Goldberg, M. E., Colby, C. L. & Duhamel, J (1990). Representation of visuomotor space in the parietal lobe of the monkey. *CSH Symposium in Quantitative Biology*. 55, 729-740
- Helmholtz, H. L. F. von (1910). *Treatise on Physiological Optics*. Translated by J. P. Southall, 1925. New York: Dover.
- Kanizsa, G. (1979). *Organization in vision*. New York, Praeger.
- Maunsell, J. H. R. & Van Essen, D. (1983). Functional properties of neurons in the middle temporal visual area of the macaque monkey. I. Selectivity for stimulus direction, speed, and orientation. *Journal of Neurophysiology*, 49, 1127-1147.
- Michotte, A., Thines, G., & Crabbe, G. (1964). *Les complements amodaux des structures perceptives*. Louvain: Publications Universitaires de Louvain.
- Snyder, L. H., Batista, A. P. & Andersen, R. A. (1997). Coding of intention in the posterior parietal cortex. *Nature*, 386, 167-170
- Wetherill, G. B. & Levitt, H. (1965). Sequential estimation of points on a psychometric function. *British Journal of Mathematical and Statistical Psychology*, 18, 1-10.
- Yantis, S. (1995). Perceived continuity of occluded visual objects. *Psychological science*, 6, 182 - 185.

Index Autor Kap. 4

- Andersen, R. A. 63, 65
Assad, J. A. 53, 54, 65
Barash, S. 63, 65
Barnes, G. R. 64, 65
Batista, A. P. 65
Bracewell, R. M. 63, 65
Bushnell, M. C. 63, 65
Colby, C. L. 63, 64, 65
Crabbe, G. 54, 65
Duhamel, J.-R. 63, 65
Fogassi, L. 63, 65
Gnadt, J. W. 63, 65
Goldberg, M. E. 63, 65
Helmholtz, H. L. F. von 65
Kanizsa, G. 65
Levitt, H. 56, 65
Maunsell, J. H. R. 53, 54, 60, 63, 65
Michotte, A. 54, 65
Robinson, D. L. 63, 65
Snyder, L. H. 54, 65
Southall, T. L. 65
Thines, G. 54, 65
Vaina, L. M. 53
van Essen, D. C. 60, 63, 65
Wetherill, G. B. 56, 65
Yantis, S. 54, 65